6. K. L. Hardee and A. J. Bard, *This Journal*, **122**, 739 (1975).
7. L. A. Harris and R. H. Wilson, *ibid.*, **123**, 1010 (1976).
8. J. F. Houlihan, D. P. Madacsi, E. J. Walsh and L. N. Mulay, *Mater. Res. Bull.*, **11**, 1191 (1976).
9. L. A. Harris, D. R. Cross, and M. E. Gerstner, *This Journal*, **124**, 839 (1977).
10. M. Gleria and R. Memming, *J. Electroanal. Chem. Interfacial Electrochem.*, **65**, 163 (1975).
11. R. Pettinger, H. R. Schöppel, and H. Gerischer, *Ber. Bunsenges. Phys. Chem.*, **80**, 849 (1976).
12. T. Moeller, "Inorganic Chemistry," p. 301, John Wiley & Sons, New York (1952).
13. C. E. Mortimer, "Chemistry, A Conceptual Approach," 2nd ed., p. 769, Van Nostrand Reinhold Company, New York (1971).
14. A. B. Ellis, S. W. Kaiser, and M. S. Wrighton, *J. Am. Chem. Soc.*, **98**, 1635 (1976).
15. G. Hodes, J. Manassen, and D. Cahen, *Nature*, **261**, 403 (1976).
16. B. Miller and A. Heller, *Nature*, **262**, 680 (1976).
17. J. E. Huheey, "Inorganic Chemistry, Principles of Structure and Reactivity," Table 7-6, Harper and Row Publishers, New York (1972).

Semiconductor Electrodes

XIX. An Investigation of S/Se Substitution in Single Crystal CdSe and CdS Photoelectrodes by Electron Spectroscopy

Rommel N. Noufi,* Paul A. Kohl,* James W. Rogers, Jr., John M. White, and Allen J. Bard**

Department of Chemistry, The University of Texas at Austin, Austin, Texas 78712

ABSTRACT

Photoelectron spectroscopy studies verify the occurrence of S/Se substitution in single crystal CdSe and CdS photoanodes when used in photoelectrochemical cells containing S^{2-} or Se^{2-} solutions. A possible mechanism of the S/Se exchange is discussed as well as its consequences on the electrode stability and the output parameters of the photoelectrochemical cells.

A number of studies have shown that cadmium chalcogenide photoelectrodes can be stabilized in aqueous solutions by the addition of sulfide, selenide, or telluride ions (1-3). This stabilization is attributed to the favorable redox potential of the X/X^{2-} couple (X = S, Se, Te) (4, 5) compared to the potential where electrode oxidation can occur or the preferential adsorption of sulfide ions for the case of CdS. Recently (6), the behavior of mixed CdS/CdSe solid solution photoelectrodes in polysulfide solutions was described, where changes in the flatband potential and bandgap with variations in the S/Se ratio were observed.

Although CdS and CdSe show quite stable operation in sulfide and selenide electrolytes, changes in the photocurrent with time are observed and indeed one would expect from thermodynamic reasoning that exchange of solution chalcogenide ions with semiconductor lattice ions would occur. Recent reports (7-9) indeed have provided evidence for such substitution. Thus Cahen *et al.* (7) showed by x-ray photoelectron spectroscopy (XPS or ESCA) that sulfide substitution occurs on polycrystalline CdSe. Similarly Heller *et al.* (8) found evidence of S substitution in CdSe by Auger electron spectroscopy (AES) and electron beam luminescence. Gerischer and Gobrecht (9) also proposed that changes occur in the surface of CdS and CdSe single crystals under illumination in sulfide electrolytes based on changes in the photocurrent spectra and Mott-Schottky plots with operation time.

We report here detailed AES and XPS studies of the surface changes which occur in single crystal CdS and CdSe photoanodes when used in photoelectrochemical cells (PEC). The results show that Se substitution occurs in the CdS/Se^{2-} system and S substitution occurs in the $CdSe/S^{2-}$ system and provide information about the mechanism of stabilization and its effect on the output parameters of the PEC.

Experimental

The electrochemical cells, light sources, method of electrode preparation, and instrumentation were the same as those previously described (6). Both single crystals (Cleveland Crystals, Cleveland, Ohio) and the polycrystalline powder (Ventron, Beverly, Massachusetts) were of high purity (99.999+%). We showed that the CdS was Se-free and the CdSe was S-free, as specified by the manufacturers, by AES and XPS analysis. Surface treatment carried out prior to use involved polishing of the single crystals with 6 μm alumina to a mirror finish followed by a chemical etch. The CdS crystals were etched in 6*M* HCl for 30 sec followed by rinsing with deionized water, while the CdSe crystals were etched for 30 sec in concentrated HNO_3 followed by rinsing with a 0.1*M* KCN solution to dissolve any Se formed during etching, then followed by rinsing with deionized water. Na_2S and Na_2Se solutions were prepared from analytical grade reagents. The Na_2Se solutions were obtained by bubbling H_2Se into a 1*M* NaOH solution under nitrogen. The Na_2S solution was filtered twice then deaerated and stored under nitrogen. All experiments were performed under positive nitrogen pressure. Stirring was accomplished with a magnetic stirrer. After performing the photoelectrochemical experiments, the electrodes were rinsed with 1*M* Na_2S solution followed by copious amounts of deaerated deionized water.

PEC experiments were run with the electrodes potentiostated at −0.5V *vs.* SCE using a large Pt counter-electrode (~10 cm^2). The photocurrents produced under illumination with white light (intensities of 20-180 mW/cm^2) were 2-43 mA/cm^2. The electrodes were employed as photoanodes for different amounts of photocharge passing through the electrode surface and compared to electrodes that were immersed at open circuit in the appropriate solution.

Thin films (~500Å) of both CdSe and CdS on platinum foils (1.5 × 1.5 cm) were prepared by vacuum evaporation of the powders from a hot tungsten filament. The film thickness was determined with a Sloan Model 200 Thickness Monitor (Santa Barbara, California). These films were used to calibrate the sputtering rate of CdS and CdSe by the argon ion beam in the electron spectroscopy analysis.

AES and XPS analyses were performed with a Physical Electronics Model 548 Spectrometer (Eden Prairie,

* Electrochemical Society Student Member.
** Electrochemical Society Active Member.
Key words: ESCA, energy conversion, photoelectricity.

Minnesota). A 5 kV, 10-15 μA, focused electron beam was used to excite the substrate during AES measurements. While depth profiling, the voltage ramp was multiplexed such that the S(LMM) (152 eV), C(KLL) (272 eV), Cd(MNN) (376 eV), and Se(LMM) (1315 eV) transitions could be sequentially scanned in less than 1 min. The argon ion beam used for sputter etching was operated at 5 kV and 30 mA emission yielding a uniform beam with a current density of 3.55 μA/cm^2. The cross-sectional area of the circular sputtered crater was approximately 0.13 cm^2. XPS measurements were taken utilizing both Al Kα and Mg Kα anodes. The data were collected digitally using pulse counting and signal averaging techniques. Both broad scan 0-1000 eV binding energy (resolution = 1.6 eV FWHM) and high resolution (0.8 eV FWHM) XPS analysis were carried out on the samples as a function of sputter time. During the sputtering process the ion pump was turned off and the vacuum chamber backfilled to 1×10^{-5} Torr in Ar. While making XPS measurements the background pressure was maintained in the 5×10^{-9}-5×10^{-8} Torr range. Residual gas analysis showed the major contaminants to be H_2O and CO at these pressures. The intensity of a XPS transition is proportional to the peak area and can be expressed as

$$I = I_0\, n\sigma\lambda(\epsilon)\, D(\epsilon)$$

where I_0 = x-ray flux, n = atomic density, σ = cross section for ionization, $\lambda(\epsilon)$ = mean free path of the escaping electron, and $D(\epsilon)$ = the detector efficiency. The ratio of intensities for two elements can then be expressed (10) as

$$\frac{I_a}{I_b} = \frac{n_a}{n_b}\left(\frac{\sigma_a\lambda_a D_a}{\sigma_b\lambda_b D_b}\right) = \frac{n_a}{n_b}(Y)$$

The expression in parenthesis remains constant to a first approximation for a given matrix and thus can be determined empirically from standard samples. Both high purity pressed powders and clean single crystals were used to determine Y. Ratios of atomic densities could then be derived from intensity ratios. Using the same standards, relative Auger sensitivities were determined from peak-to-peak height ratios.

Sputtering rates were calibrated by depth profiling CdS and CdSe films of known thickness. The Cd (376 eV), S (152 eV), and Pt (237 eV) peaks were monitored while sputtering; the sputtering process was judged complete when the Cd and S signals were reduced to the noise level. Two profiles were run on each film, the craters being well isolated on opposite sides of the film as judged visually by the bright, shiny platinum at the crater bottom. By this method, sputtering rates for CdS and CdSe of 16 $\pm$ 3 and 19 $\pm$ 3 Å/min, respectively, were found. This corresponds to a sputtering efficiency of 2.4 molecules/ion for CdS and 2.6 molecules/ion for CdSe. A constant Cd/Se Auger peak-to-peak height ratio during the sputtering process indicated that Cd and Se were removed from the surface region at the same rate. Overlap of a platinum transition with the S (152 eV) peak precluded any such determination on CdS. The fact that the CdS and CdSe sputtering rates are the same within experimental error indicates that preferential sputtering is not significant.

Results

CdSe single crystals.—Three CdSe single crystals were examined by electron spectroscopy after various pretreatments. One crystal was soaked in 1*M* NaOH, 1*M* Na_2S, 1*M* S solution for 30 min at open circuit under illumination; the other two crystals were used as photoanodes in a PEC with a total charge passed of 2.5 and 12.0 C/cm^2 in a similar solution. Initial AES and XPS analysis after immersion and transfer to the spectrometer showed large amounts of C with lesser amounts of O on all of the crystals. The open-circuit crystal showed a small amount of S on the surface which was completely removed with less than 1 min of Ar$^+$ bombardment. The C signal was also reduced to its background level with this same amount of sputtering. Whether this S is substituted, as suggested by Heller *et al.* (8) or merely adsorbed on the surface cannot be ascertained from our data but it is evident that S is only present in the first few atomic layers. A large amount of S was found in the surface region on the crystal which had been anodized for 2.5 C/cm^2. The ratios of AES peak-to-peak heights for Cd/Se, S/Cd, and Se/S as a function of sputter depth given in Fig. 1, suggest that sulfur is substituted to a depth of 40Å which corresponds to about 12 atomic layers. The high resolution XPS spectra of the S (2s)-Se (3s) and S (2p)-Se (3p) regions after 0.5 and 8 min of sputtering are given in Fig. 2 and 3. Contributions from both Se and S are evident after 0.5 min of sputtering but the S signal is completely gone after 8 min. The C signal on this sample was reduced to its background level by less than 1 min of sputtering. The CdSe crystal which was anodized for 12 C/cm^2 showed S substitution to a depth of about 67Å or 20 atomic layers as shown by the atomic ratios of S/Cd, Cd/Se, and Se/S *vs.* sputter depth for this crystal (Fig. 4). The solid lines are from AES peak-to-peak height ratios corrected for elemental sensitivity as determined from the standard samples. In addition to the crystal which was anodized for 12

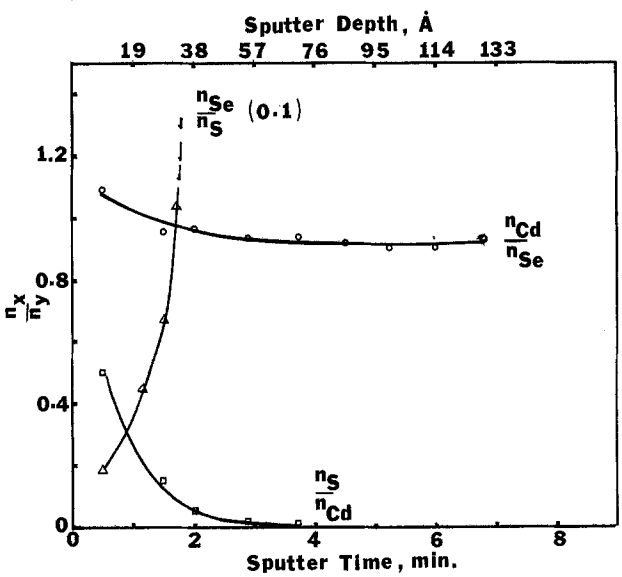

Fig. 1. Atomic ratios of Se/S, Cd/Se, and S/Cd from AES peak-to-peak ratios as a function of sputter depth for a CdSe single crystal electrode photoanodized in a 1M NaOH, 1M Na_2S, 1M S solution (2.5 C/cm^2).

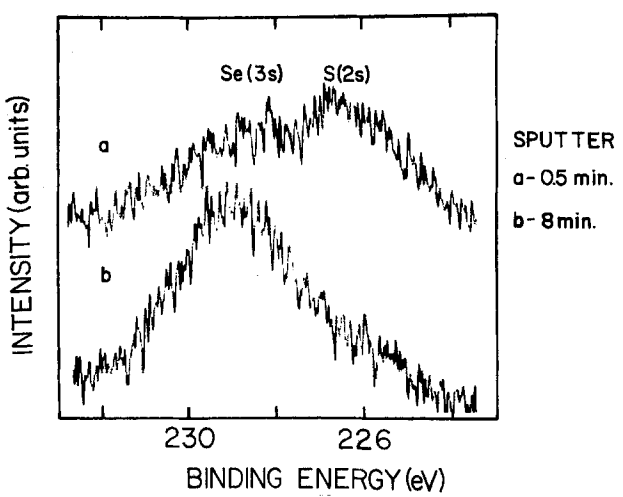

Fig. 2. High resolution XPS spectra of the S (2s)-Se (3s) region of the same CdSe electrode in Fig. 1 as a function of sputter time.

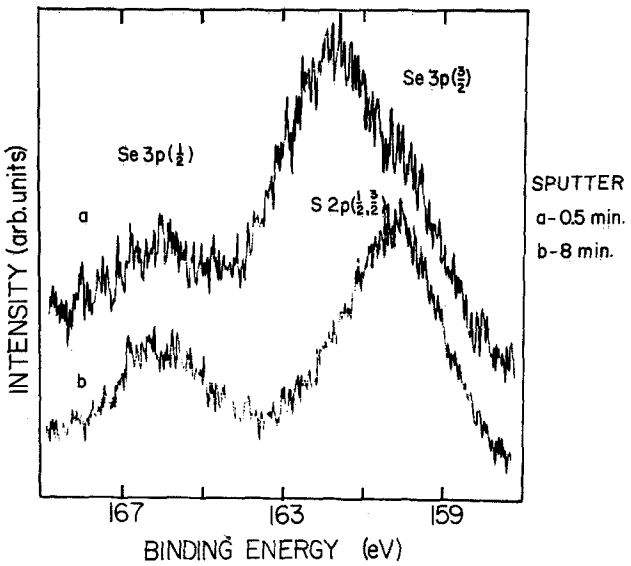

Fig. 3. High resolution XPS spectra of the S (2p)-Se (3p) region of the same CdSe electrode in Fig. 1 as a function of sputter time.

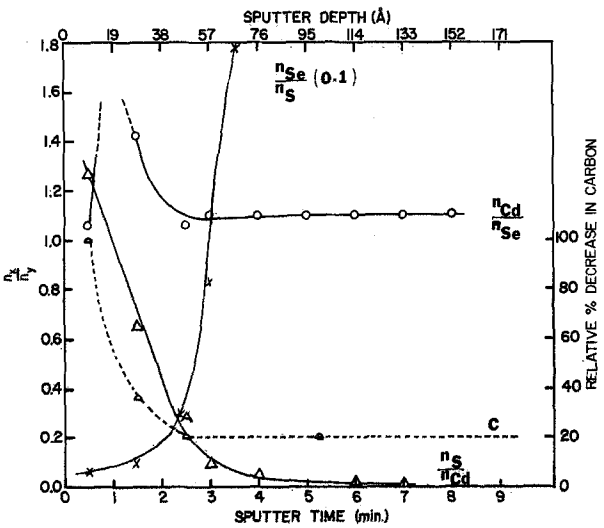

Fig. 4. Atomic ratios of Se/S, Cd/Se, and S/Cd from AES peak-to-peak ratios as a function of sputter depth. Electrode and solution as in Fig. 1 (12 C/cm²).

C/cm² in 1*M* Na_2S, another CdSe crystal was anodized under the same conditions except the solution was also 0.05*M* in dissolved Se. This has been shown to decrease the rate of current decay of CdSe photoanodes in S^{2-} media under extended electrolysis (8). A plot of the AES results for this anode in Fig. 5 (compared to Fig. 4) indicates S substitution to a depth of 33Å. Besides the usual contaminants of C and O, traces of Na and SiO_2 were initially present on the surface of this crystal. The Na probably arises from the Na_2S solution itself and the trace of SiO_2 could originate from the silicone rubber sealant used to isolate the rear portions of the crystal from the solution, or from attack of the alkaline solutions on the Pyrex cells.

CdS.—CdS single crystals were pretreated in a manner similar to the CdSe crystals. One was immersed at open circuit for 30 min in 1*M* NaOH, 0.5*M* Na_2Se, 0.5*M* Se solution while two others were anodized in a similar solution for times equivalent to 0.5 and 6 C/cm². Again C and O were initially observed on the surface of all of these crystals. The small amount of Se initially present on the open-circuit sample again was removed in less than 1 min of sputtering indicating no Se substitution beyond the surface region. The crystal which had been anodized for 0.5 C/cm² showed a layer of

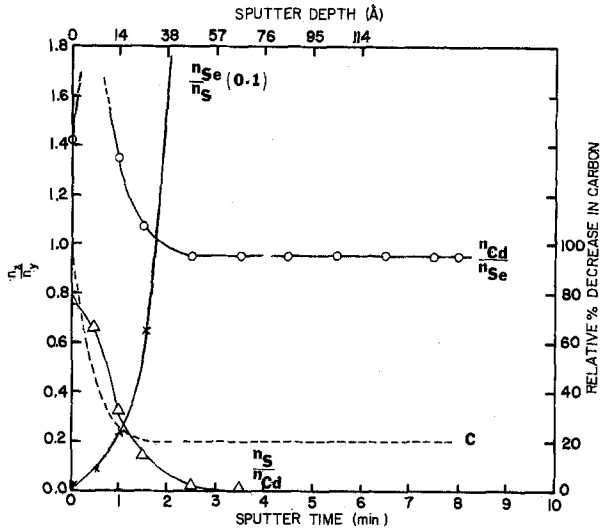

Fig. 5. As Fig. 4 except for a solution also containing 0.05*M* Se

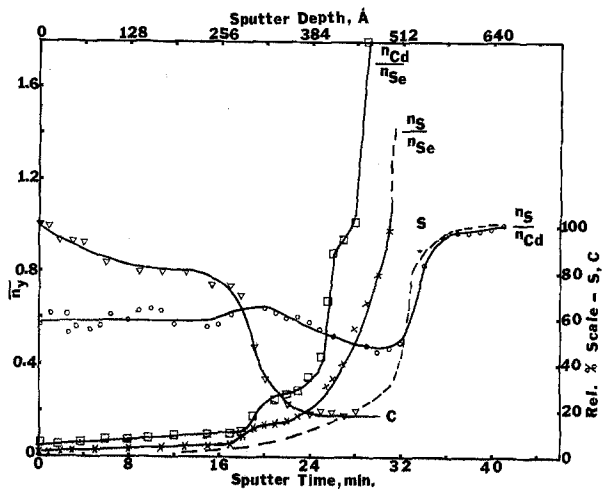

Fig. 6. Atomic ratios of S/Se, Cd/Se, and S/Cd from AES peak-to-peak ratios as a function of sputter depth for a CdS single crystal photoanodized in 1*M* NaOH, 0.5*M* Na_2Se, 0.5*M* Se solution (0.5 C/cm²).

pure Se 250Å deep, followed by a region of Se substitution into the CdS about 240Å in depth.

This Se overlayer was highly contaminated with C as seen from Fig. 6. The C was essentially reduced to its background level as the region of substitution was approached. We define the region of substitution in this crystal to begin where the Cd and S signals first appear. The S (2p)-Se (3p) and Se x-ray induced regions as a function of sputter time for the 6 C/cm² crystal are shown in Fig. 7. The Se x-ray induced Auger transition, which appears at a binding energy of 178 eV when an Al $K\alpha$ anode is used for excitation, is also shown. Even after this sample was sputtered for a total of 51 min Se could still be detected, as shown in Fig. 7. This indicates that Se substitution occurs deep into the bulk, greater than 800Å in this case. The results on both CdSe and CdS crystals are summarized in Table I.

Table I. Summary of the extent of S/Se substitution for the CdS and CdSe photoelectrodes under different operating conditions

CdSe/S^{2-} (A)			CdS/Se^{2-} (A)		
Open circuit	2.5 C/cm²	12 C/cm²	Open circuit	0.5 C/cm²	6 C/cm²
<12	~40	67 (33Å-Se)	<12	240	>800

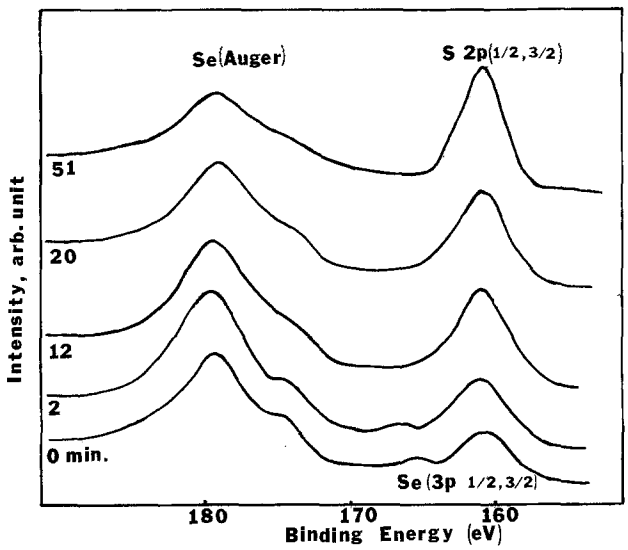

Fig. 7. High resolution spectra of the S(2p)-Se(3p) and x-ray induced Auger transition as a function of sputter time. CdS single crystal photoanodized in a 1M NaOH, 0.5M Na_2Se, 0.5M Se solution (6 C/cm^2).

Discussion

It is clear from the results that S/Se substitution takes place in both systems, *i.e.*, from a polysulfide solution into the CdSe photoanode and from the polyselenide solution into the CdS photoanode. The extent of substitution of Se into CdS is greater than S into CdSe, as indicated by the relative depth of penetration. The solubility product constants for CdS and CdSe are 5×10^{-28} and 1×10^{-31}, respectively, as calculated from thermodynamic data (11). That the substitution of the anion is greatly enhanced on the passage of charge under illumination is clear from the data given in Table I. The exchange could occur via some initial photo-oxidation of the CdS and CdSe electrodes in a manner suggested by several investigators (4, 12), followed by reprecipitation of the Cd^{2+}

$$\underline{CdSe} + 2p^+ \rightarrow Cd^{2+} + \underline{Se} \quad [1]$$

$$\underline{Se} + S^{2-} \rightarrow SSe^{2-} \quad [2]$$

$$Cd^{2+} + S^{2-} \rightarrow \underline{CdS} \quad [3]$$

and

$$\underline{CdS} + 2p^+ \rightarrow Cd^{2+} + \underline{S} \quad [4]$$

$$\underline{S} + Se^{2-} \rightarrow SSe^{2-} \quad [5]$$

$$Cd^{2+} + Se^{2-} \rightarrow \underline{CdSe} \quad [6]$$

Because of the high concentration of the anion in solution the Cd^{2+} will precipitate very quickly as CdS or CdSe. The pure Se layer found in one of the CdS samples can probably be attributed to slow kinetics in [2], as also found by Ellis *et al.* (13). The newly formed material will probably possess a more polycrystalline character of different composition, as suggested by Gerischer and Gobrecht (9). A 600-magnification SEM picture (Fig. 8) clearly shows the change in the surface nature of a CdS electrode before and after anodization in a polyselenide solution. The increased roughness and graininess of the surface probably indicates a regenerated one by the reprecipitation of CdSe to give a surface containing both anions and exhibiting a polycrystalline character with a different doping level, resistivity, adsorption characteristics toward the anions in solution, and electron affinity. We have recently described the behavior of CdS-CdSe solid solution electrodes (6) and showed that the flatband potential and open-circuit voltage changed with electrode composition. We attributed this behavior to a change in the electron affinity with the change in composition of the

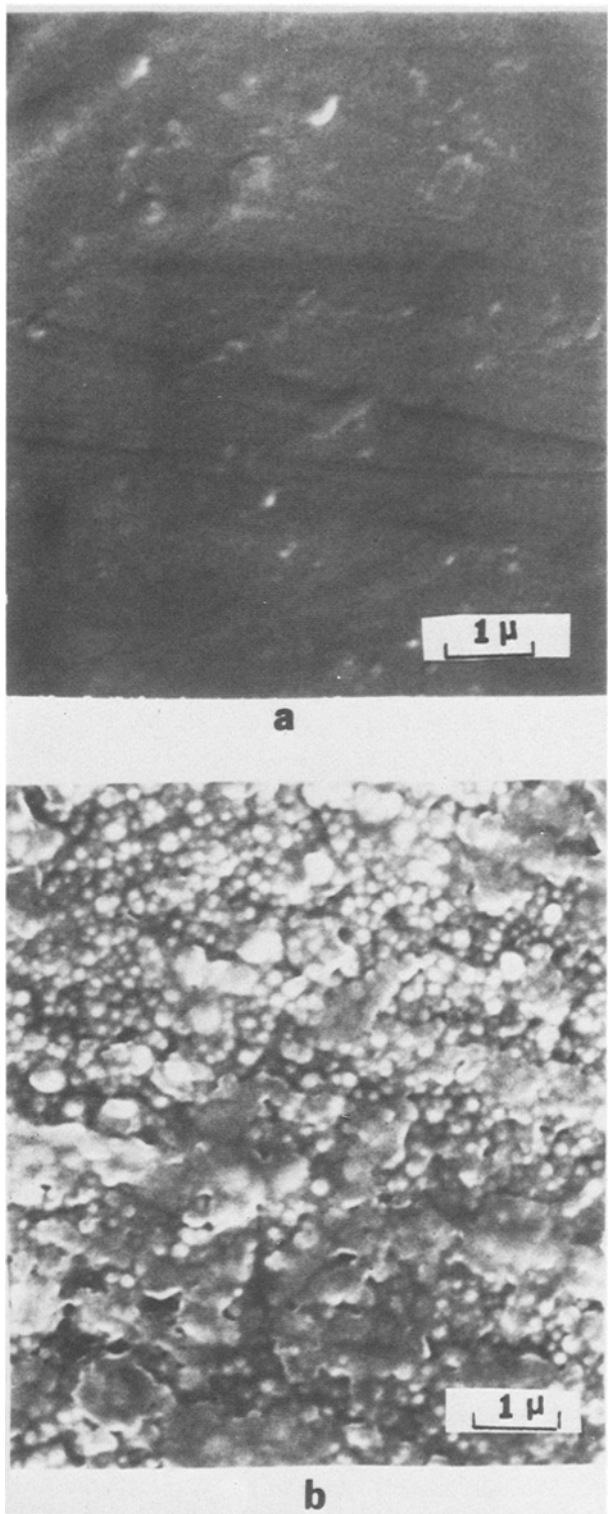

Fig. 8. SEM pictures showing the change in the surface nature of a CdS single crystal electrode: (a) before photoanodization, (b) after the passage of 0.2 C/cm^2 photocharge in a solution as in Fig. 7.

anions. Just as the open-circuit voltage (V_{oc}) increased with the above solid-solution electrodes as the composition of one of the anions was increased, a similar change in the V_{oc} was observed with the CdS and CdSe photoanodes as the anion substitution proceeded.

The short-circuit current of these electrodes has been shown by several groups (7, 8), and was confirmed in this laboratory, to decrease with operation time. The rate of the initial decrease was greater for higher intensities (routinely, initial currents of 5 to 40 mA/cm^2 corresponding to 50 to 180 mW/cm^2 white light intensities). Typical behavior of the photocurrent for a

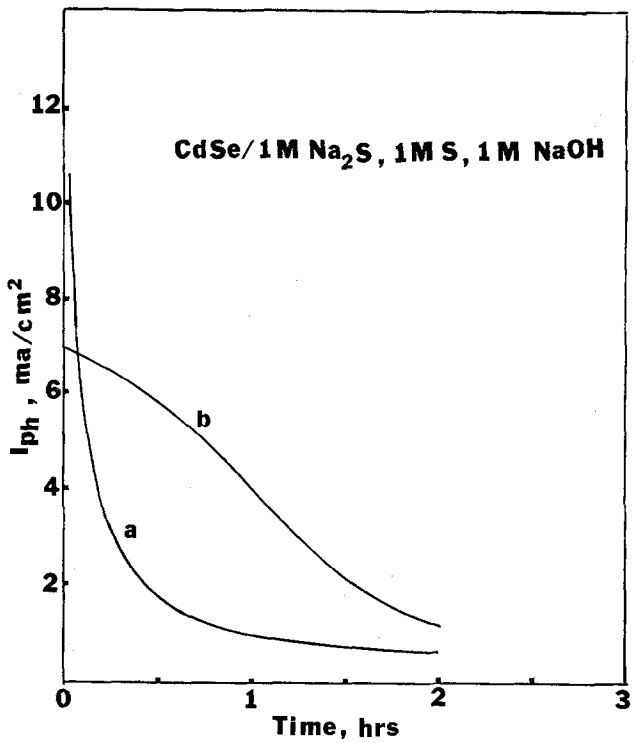

Fig. 9. Photocurrent vs. time for a CdSe photoanode operated in a two electrode photoelectrochemical solar cell employing a solution as in Fig. 1. White light illumination intensity: (a) about 180 mW/cm^2, (b) about 50 mW/cm^2.

CdSe operated in a polysulfide solution is shown in Fig. 9. This deactivation can be rationalized in terms of the energy level diagram one can establish for these substituted electrodes. If the operation of these electrodes is carried long enough so that a substituted layer is formed at the surface of the electrode, the energy level diagram for equilibrium condition will be as shown in Fig. 10 for a CdS layer on CdSe electrode and in Fig. 11 for CdSe on CdS. The relative position of the conduction bands for both materials was taken from the electron affinities. From Fig. 10 one sees that a layer of larger bandgap n-type semiconductor on a similar semiconductor of smaller bandgap will tend to inhibit the passage of holes to the surface and the flow of electrons into the bulk. In the opposite situation, *i.e.*, a CdSe layer on a CdS electrode, the flow of holes to the surface is favorable, however the flow of electrons into the bulk is inhibited as seen in Fig. 11. The magnitude of the barrier is progressively changing as x changes in the $CdSe_{1-x}S_x$ and $CdS_{1-x}Se_x$ with operation time, where $x = 1$ means formation of a substituted layer. Other factors to be considered are a lattice mismatch between CdS and CdSe and the possibility of defects at the surface of the newly formed layer which creates traps and thus sites for carrier recombination.

Recently, Heller and co-workers (8) showed that the current blockage in a CdSe electrode can be reduced or eliminated by maintaining an adequate amount of dissolved selenium in the polysulfide solution which resulted in maintaining adequate selenium concentration in the surface film. In this work the results as shown in Fig. 5 indicate that substitution of S for Se into a CdSe electrode operated in a selenium-containing polysulfide solution is appreciably reduced.

In summary, we show in this work that although CdS and CdSe are stable against photodissolution in polysulfide and polyselenide solutions, the latter contribute, through anion substitution, to the deterioration of the output parameters, with time of operation.

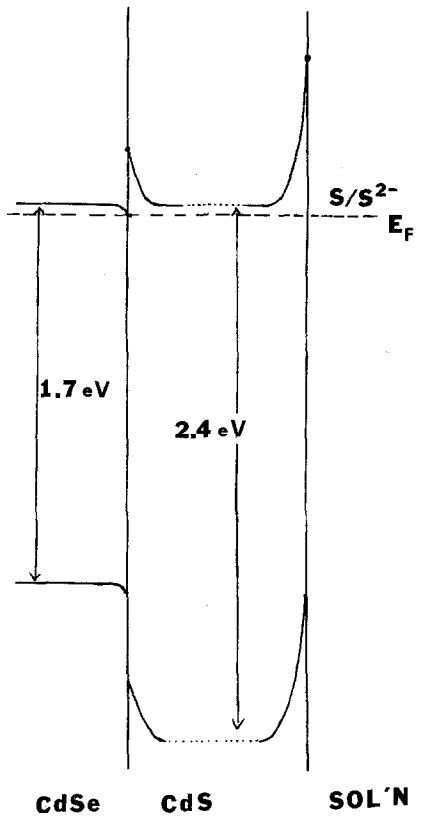

Fig. 10. Energy band diagram, at equilibrium in the dark, of an n-CdSe electrode with an n-CdS layer in contact with a polysulfide solution.

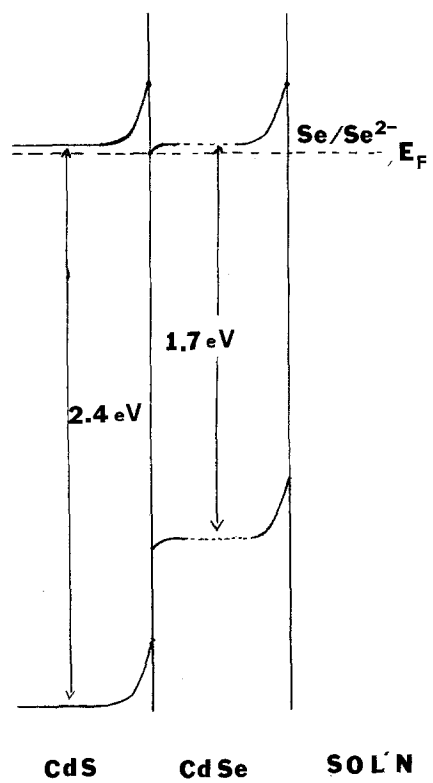

Fig. 11. Energy band diagram, at equilibrium in the dark, of an n-CdS electrode with an n-CdSe layer in contact with a polyselenide solution.

Acknowledgment

The support of this research by the National Science Foundation (to A.J.B.) and the Office of Naval Research (to J.M.W.) is gratefully acknowledged. The electron spectroscopy instrumentation was purchased from funds from a grant to The University of Texas at Austin by the National Science Foundation (CHE 76-

05172). We appreciate the helpful suggestions of Drs. Gary Hodes, Joost Manassen, and David Cahen of the Weizmann Institute and the cooperative efforts of this group in this area under a U.S.-Israel Binational Science Foundation grant.

Manuscript submitted Sept. 14, 1978; revised manuscript received Nov. 20, 1978.

Any discussion of this paper will appear in a Discussion Section to be published in the December 1979 JOURNAL. All discussions for the December 1979 Discussion Section should be submitted by Aug. 1, 1979.

Publication costs of this article were assisted by The University of Texas at Austin.

REFERENCES

1. (a) A. B. Ellis, S. W. Kaiser, and M. S. Wrighton, *J. Am. Chem. Soc.*, **98**, 1635 (1976); *ibid.*, **98**, 6418 (1976). (b) A. B. Ellis, S. W. Kaiser, J. M. Bolts, and M. S. Wrighton, *J. Am. Chem. Soc.*, **99**, 2839 (1977).
2. G. Hodes, J. Manassen, and D. Cahen, *Bull. Isr. Phys. Soc.*, **22**, 100 (1976); *Nature*, **261**, 403 (1976).
3. (a) B. Miller and A. Heller, *Nature*, **262**, 680 (1976). (b) A. Heller, K. C. Chang, and B. Miller, *This Journal*, **124**, 697 (1977). (c) B. Miller, A. Heller, M. Robbins, S. Menezes, K. C. Chang, and J. Thompson, Jr., *ibid.*, **124**, 1019 (1977).
4. A. J. Bard and M. S. Wrighton, *ibid.*, **124**, 1706 (1977).
5. H. Gerischer, *J. Electroanal. Chem.*, **82**, 133 (1977).
6. R. N. Noufi, P. A. Kohl, and A. J. Bard, *This Journal*, **125**, 375 (1978).
7. D. Cahen, G. Hodes, and Joost Manassen, *This Journal*, **125**, 1623 (1978).
8. A. Heller, J. P. Schwartz, A. G. Vadimsky, S. Menezes, and B. Miller, *This Journal*, **125**, 1156 (1978).
9. H. Gerischer and J. Gobrecht, *Ber. Bunsenges. Phys. Chem.*, **82**, 520 (1978).
10. R. B. Shalvoy and P. J. Reucroft, *J. Elect. Spectrosc. Relat. Phenom.*, **12**, 351 (1977).
11. (a) D. D. Wagman, W. H. Evans, V. B. Parker, I. Halow, S. M. Bailey, and R. H. Schum, NBS Tech. Note 270-3 (1968). (b) J. Drowarf and P. Goldfinger, *J. Chim. Phys.*, **55**, 721 (1958). (c) P. Goldfinger and M. Jeunehomme, *Trans. Faraday Soc.*, **59**, 2851 (1963).
12. (a) H. Gerischer and W. Minalt, *Electrochim. Acta*, **13**, 1239 (1968). (b) H. Gerischer, *J. Electroanal. Chem.*, **58**, 263 (1975). (c) H. Gerischer, *ibid.*, **82**, 133 (1977).
13. A. B. Ellis, S. W. Kaiser, and M. S. Wrighton, *J. Am. Chem. Soc.*, **98**, 6855 (1976).

Effects of Cations on the Performance of the Photoanode in the n-GaAs | K_2Se-K_2Se_2-KOH | C Semiconductor Liquid Junction Solar Cell

B. A. Parkinson,* A. Heller, and B. Miller****

Bell Laboratories, Murray Hill, New Jersey 07974

ABSTRACT

Cations adsorbed on n-GaAs affect the fill factor and the open-circuit voltage of the n-GaAs |0.8*M* K_2Se-0.1*M* K_2Se_2-1*M* KOH|C cell. An AM1 solar-to-electrical conversion efficiency of 12% is reached by chemisorbing Ru(III) on the photoanode. This efficiency is maintained upon passage of 35,000 C/cm^2. The effect of Ru(III) is interpreted as a reaction with a surface chemical entity associated with a surface state near the conduction band, which shunts the cell by allowing electrons to tunnel through the barrier at the junction. Reaction with Ru(III) converts the shunting surface state to one to which electrons cannot tunnel. Being strongly adsorbed, Ru(III) also reduces the effect of certain impurities such as Bi(III) which otherwise decrease the power output.

Photoelectrochemical cells based on semiconductor liquid junctions have reached significant solar-to-electrical power conversion efficiency in the short period since their suggestion (1). The n-GaAs|$Se^{=}$-$Se_x^{=}$-OH^-|C cell was initially reported by this laboratory to achieve 8.8% efficiency under 75 mW/cm^2 insolation (2). The operating parameters of this cell suggested that further improvement would be attainable if variables associated with the GaAs surface could be better understood and controlled. This expectation has been realized by surface modification procedures leading to a 12% efficiency at 100 mW/cm^2 solar intensity (3). In this paper, we detail the voltammetric characteristics of the surface enhancement steps, the stability of the improved output, and a mechanistic interpretation of these effects.

Until this recent development of semiconductor liquid junction solar cells, relatively little attention was paid to the semiconductor surface pretreatment. However, there is considerable historical precedent, which we cannot review with proper attention in this space, for expecting this to be important. Brattain and Boddy showed that surface preparation (4-6) and adsorbed impurity cations (4, 5) and anions (6) modify interface states at semiconductor liquid junctions. The effects of such states on the redox processes at illuminated semiconductors have been reviewed by Gerischer (7) and Morrison (8). In the recent context of semiconductor redox couple systems, Frank, Kohl, and Bard (9, 10) attributed voltammetric deviations from expected behavior to the presence of interface states at junctions in nonaqueous electrolytes as well. Effects of surface condition have been observed by spectroscopic techniques and from the output of the cells (11, 12). Indeed, recent improvements in the n-GaAs|$Se^{=}$-$Se_x^{=}$-OH^- junction behavior have been accomplished by controlling the chemistry and topography of the electrode surface (3).

The chemical nature of the semiconductor surface during its operation as a solar cell anode is the result of surface treatment reactions prior to cell electrolyte immersion, and any subsequent chemical modification, including electrochemical reactions accompanying its

* Electrochemical Society Student Member.
** Electrochemical Society Active Member.
Key words: photoelectrochemistry, energy conversion, surface treatment.